

Manufacturing and integration of the IRDIS dual imaging camera and spectrograph for SPHERE

Kjetil Dohlen^a, Michael Carle^a, Fabrice Madec^a, Maud Langlois^b, David Le Mignant^a,
Michel Saisse^a, Arthur Vigan^a, Gilles Arthaud^a, Rudy Barette^a, Jean-Antoine Benedetti^a,
Jean-Claude Blanc^a, Patrick Blanchard^a, William Bon^a, Louis Castinel^a, Christophe Fabron^a,
Lucien Hill^a, Marc Jaquet^a, Philippe Laurent^a, Marc Llored^a, Nataly Manzone^a, Silvio Mazzanti^a,
Jeanne Melkonian^a, Gabriel Moreaux^a, Claire Moutou^a, Alain Origne^a, Markus Feldt^c,
Vianak Naranjo^c, Ralf-Rainer Rohloff^c, Jean-Luc Beuzit^d, Laurence Gluck^d, David Mouillet^d,
Pascal Puget^d, Andrea Baruffolo^e, Francois Wildi^f, Reinhold Dorn^g, Gert Finger^g, Norbert Hubin^g,
Markus Kasper^g, Jean-Louis Lizon^g

^a Laboratoire d'Astrophysique de Marseille UMR 6110, CNRS/Université de Provence, 38 rue Frédéric Joliot-Curie, 13388 Marseille cedex 13, France

^b CRAL, UMR 5574, CNRS, Université Claude Bernard, 9 avenue Charles André, 69561 Saint Genis Laval Cedex, France

^c Max Planck Institut für Astronomie, Königstuhl 17, D-69117 Heidelberg, Germany

^d Laboratoire d'Astrophysique de l'Observatoire de Grenoble UMR 5571, Université Joseph Fourier/CNRS, B.P. 53, F-38041 Grenoble Cedex 9, France

^e Osservatorio Astronomico di Padova, Vicolo dell'Osservatorio 5, I-35122 Padova, Italy

^f Observatoire de Genève, 51 ch des Maillettes, CH-1290 Sauverny, Switzerland

^g European Southern Observatory, Karl-Schwarzschild-Strasse 2, D-85748 Garching, Germany

ABSTRACT

SPHERE is a planet hunting instrument for the VLT 8m telescope in Chile whose prime objective is the discovery and characterization of young Jupiter-sized planets outside of the solar system. It is a complex instrument, consisting of an extreme Adaptive Optics System (SAXO), various coronagraphs, an infrared differential imaging camera (IRDIS), an infrared integral field spectrograph (IFS) and a visible differential polarimeter (ZIMPOL). The performance of the IRDIS camera is directly related to various wavefront error budgets of the instrument, in particular the differential aberrations occurring after separation of the two image beams. We report on the ongoing integration and testing activities in terms of optical, mechanical, and cryo-vacuum instrument parts. In particular, we show results of component level tests of the optics and indicate expected overall performance in comparison with design-level budgets. We also describe the plans for instrumental performance and science testing of the instrument, foreseen to be conducted during coming months.

Keywords: extrasolar planets, extreme AO, coronagraphy, dual imaging, polarimetry, long-slit spectroscopy

1. INTRODUCTION

The SPHERE (Spectro-Polarimetric High-contrast Exoplanet Research) instrument^{[1],[2]} is built by a wide consortium of European countries. It is based on an extreme AO system (SAXO)^[3] and employs coronagraphic devices^[4] for stellar diffraction suppression. It is equipped with three science channels: a differential imaging camera (IRDIS)^[5], an integral field spectrograph (IFS)^[6], and a rapid switching polarimeter (ZIMPOL)^[7].

The Infra-Red Dual-beam Imaging and Spectroscopy (IRDIS) camera provides imaging in two parallel channels over a wide field of view (FOV = 11"). A beam splitter plate associated with a mirror separates the beam in two parallel beams, focalized side-by-side onto a common detector by two identical spherical mirrors. Before reaching the detector, the beams are spectrally filtered by dual band filters (DBF) with adjacent pass-bands corresponding to sharp features in the

expected planetary spectra.^[8] Differential aberrations between the two beams are critical for the performance of the instrument,^[9] and a total budget of 10nm rms with a goal of 5nm has been fixed according to expected feasibility within reasonable cost limits.

1.1. Science case

SPHERE-IRDIS is built to discovery and study extra-solar planets by direct imaging of the circumstellar environment. The science cases are described elsewhere^{[1][2]}. The main observing mode which will be used for 80% of the time combines IRDIS dual imaging in the H band with imaging spectroscopy using the IFS in the Y-J bands by the aid of dichroic beam separation after the coronagraph. This configuration permits to benefit simultaneously from the capacities of both subsystems, in particular the large field of IRDIS (~5" radius) and the wide spectral range of the IFS. This strategy allows to reduce the number of false alarms and to confirm potential detections obtained in one channel by data from the other channel, a definitive advantage in case of detections very close to the limits of the system.

The observing modes and main characteristics are summarized in Table 1. IRDIS used alone in its various modes will allow obtaining observations in all bands from Y to short-K, either in dual imaging or in classical imaging with broad and narrow-band filters. This will be especially interesting in order to obtain complementary information on already detected and relatively bright targets (follow-up and/or characterization). Spectroscopic characterization at low or medium resolution will be possible in the long-slit mode. Additional science cases will also benefit from these observing modes (disks, brown dwarfs, etc.).^[10] This will be a very useful capability for the ESO community at a time where NACO will most likely not be offered anymore.

Table 1. Summary of IRDIS observing modes and main characteristics.

Mode	Use Science case	Wavelength Bands	Rotator mode	Filters, Resolution	Contrast Performance (1h, SNR=5, H<6)
Dual Band Imaging	Survey mode (H only) Characterization of cool outer companions	Y,J,H,Ks bands	Pupil or field stabilized	6 pairs R=20-30	$\sim 10^{-5}$ at 0.1" $\sim 10^{-6}$ at 0.5"
Dual Polarimetry Imaging	Reflected light on extended environment	Y,J,H,Ks bands	Pupil or field stabilized	4 Broad 10 Narrow bands	$\sim 10^{-4}$ at 0.1" $\sim 10^{-5}$ at 0.5" 30% circumstellar source
Slit Spectroscopy	Characterization of not too faint companions	LRS : Y-Ks MRS: Y-H	Pupil stabilized	LRS : R=50 MRS : R=500	$\sim 3 \cdot 10^{-4}$ at 0.3" $\sim 10^{-5}$ at 0.5"
Classical Imaging	Environment with no spectral features	Y,J,H,Ks bands	Pupil or field stabilized	4 Broad 10 Narrow bands	$\sim 10^{-3}$ at 0.1" $\sim 3 \cdot 10^{-4}$ at 0.5"

1.2. Performance estimations for the detection and characterization of exoplanets

The dual-band imaging (DBI) mode achieves high contrast by simultaneous imagery at both sides of the H-band methane absorption edge, allowing to remove most of the systematic speckles due to instrumental defects. Further contrast improvements has to deal with two main components: a speckle halo which is averaging over time and a quasi-static speckle pattern originating from evolving aberrations, occurring with a much longer lifetime than the atmospheric residuals.^[11] IRDIS DBI mode will allow the use of different data analysis methods to remove the speckle residuals, in

particular simultaneous Spectral Differential Imaging (SDI), for which the main limitation are the quasi-static aberrations upstream the coronagraph and the spectral separation between the DBI filters, and Angular Differential Imaging (ADI) which uses the fact that the observations are obtained in pupil-tracking mode, and for which the main limitations are the field rotation rate and the temporal evolution of the aberration. The Long Slit Spectroscopy (LSS) mode, combined with an efficient data analysis method,^[12] offers the possibility of spectral characterization of detected objects at low ($R = 60$) and medium ($R = 420$) resolutions.

Figure 1 (c) and (d) show the result of applying these data analysis methods on simulated data representing a G0 star at 10 pc with three series of planets at various angular separations. In very young systems, these planets would represent a mass of $\sim 2 M_{\text{Jup}}$ according to current evolutionary models. Figure 2 represents the 5σ detection limits that can be reached for a 4-hours observation of G0 and M0 stars with H2H3 filter pairs. Combining SDI and ADI techniques we expect to reach a contrast of $\sim 2 \cdot 10^{-5}$ at a separation of $0.2''$, which would result in the detection of $\sim 1 M_{\text{Jup}}$ planets. A detailed comparison of the performances of different data analysis methods is presented by Vigan et al. (this conference)^[13].

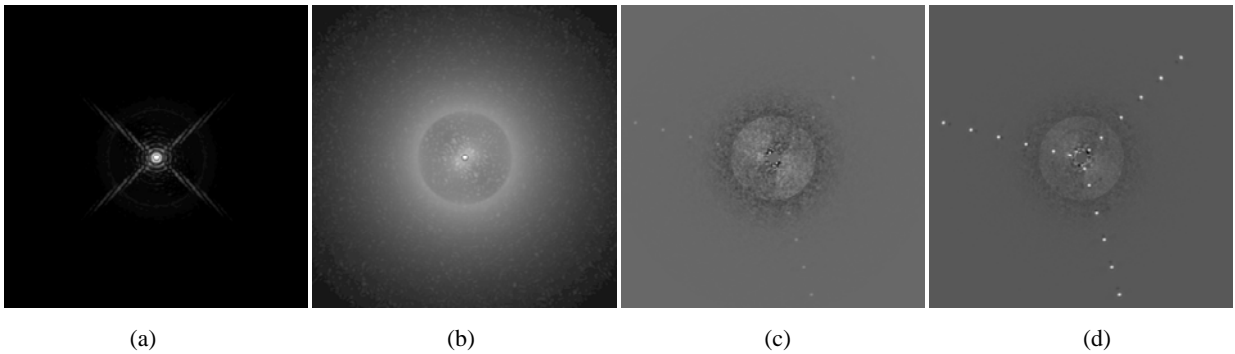


Figure 1: G0V star 10pc image with DBI (H2H3), the detected planets are located at $0.2''$, $0.5''$, $0.10''$, $1.5''$, $2.0''$, and $2.5''$ from the star and correspond to : $1.9M_{\text{J}}$ at 10My – $6.5M_{\text{J}}$ at 100My – $118.5M_{\text{J}}$ at 1Gy – $37.9M_{\text{J}}$ at 5Gy . The illustrations show the star PSF (a), the Apodized Lyot Coronagraph raw image (b), the analyzed image after using Angular Differential Imaging in filter H2 (c), and the combination of Spectral Differential Imaging (H2-H3) and Angular Differential Imaging (d). Gray scales are arbitrary.

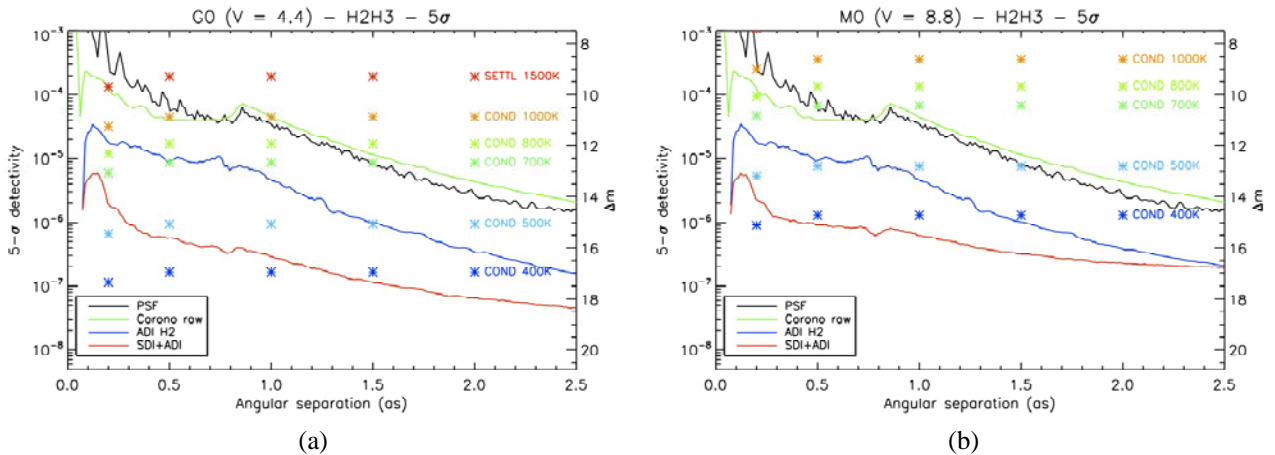


Figure 2. Some results of an extensive simulation of test cases involving various stellar ages and distances. Planetary companions intensities (crosses) are compared with radial variance profiles in the processed images with ADI and SDI+ADI data analysis methods, assuming a G0V (a) and an M0V (b) star at 10pc observed in the H2-H3 filter couple. COND refers to models for a condensed atmospheres free of dust, while SETTL refers to atmosphere models with rainout of refractory material.

2. SYSTEM ARCHITECTURE

2.1. IRDIS design

The SPHERE system^{[1][2]} consists of four subsystems: the Common Path and Infrastructure (CPI) containing an extreme adaptive optics system (SAXO) with a 40x40 actuator deformable mirror, coronagraphic systems, beam rotator, atmospheric dispersion correctors, calibration sources, etc, and the three science channels IRDIS and IFS in the infrared and ZIMPOL in the visible, see Figure 3. IRDIS^[5] is the main science module of SPHERE. Its main specifications include a spectral range from 950-2320 nm and an image scale of 12.25mas/pixel consistent with Nyquist sampling at 950nm. The FOV is 11"x12.5" in classical imaging and Ø11" in dual imaging modes. Six different dual-band imaging filter couples are defined corresponding to different spectral features in modelled exoplanet spectra. In the classical imaging mode, four broad-band filters corresponding to the atmospheric bands Y, J, H, and Ks are provided, as well as 10 narrow-band filters corresponding to molecular features and continuums. A dual polarimetric imaging mode provides simultaneous imaging in two orthogonal polarizations within any of the broad and narrow-band filters. In addition to imaging, long-slit spectroscopy at resolving powers of 50 and 500 is provided thanks to the provision of a double, zero-deviation prism and a grism. A pupil-imaging mode for system diagnosis is also implemented.

The opto-mechanical design of IRDIS is shown in Figure 4 (left). The IRDIS entrance pupil is the coronagraphic exit pupil (Lyot stop). Located in a collimated beam of diameter 10mm, it constitutes the main optical interface parameter with the common path optics. Three wheels are provided within the cryogenic environment, the common filter wheel carrying classical imaging filters, the Lyot stop wheel, and the dual imaging filter wheel. The detector is mounted on a two axis piezo motor translation stage^[14] to allow dithering for flat-field improvement. The cryostat interior is shown in Figure 4 (right). The optical bench with its cold screen is thermally strapped to a small, cylindrical LN2 tank, constantly maintained full thanks to the large LN2 tank on the side.

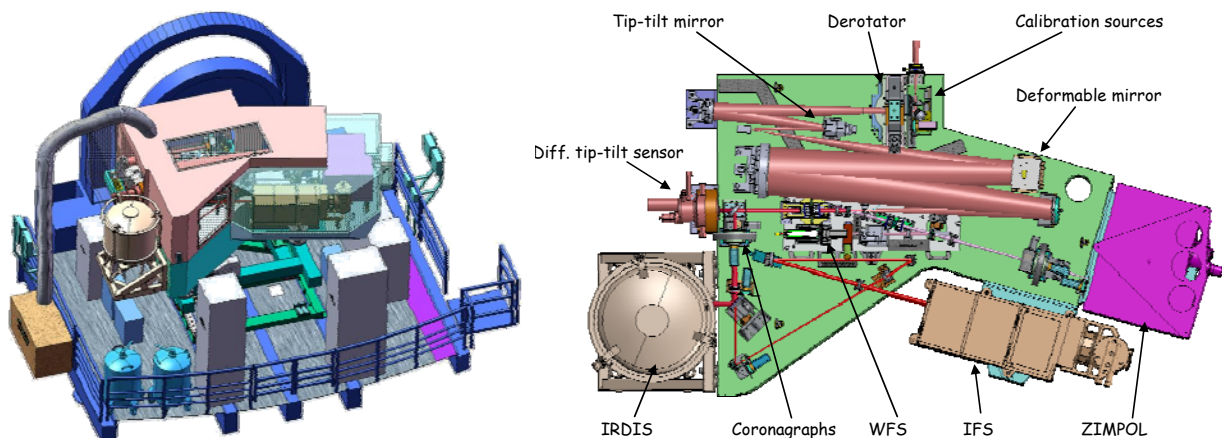


Figure 3. Global view of the SPHERE instrument as installed on the Nasmyth platform (left). IRDIS is the cylindrical cryostat attached to the left-hand side of the SPHERE optical bench. Optical layout of the common path (right), indicating how the science subsystems IRDIS (grey), IFS (beige), and ZIMPOL (violet) are alimented.

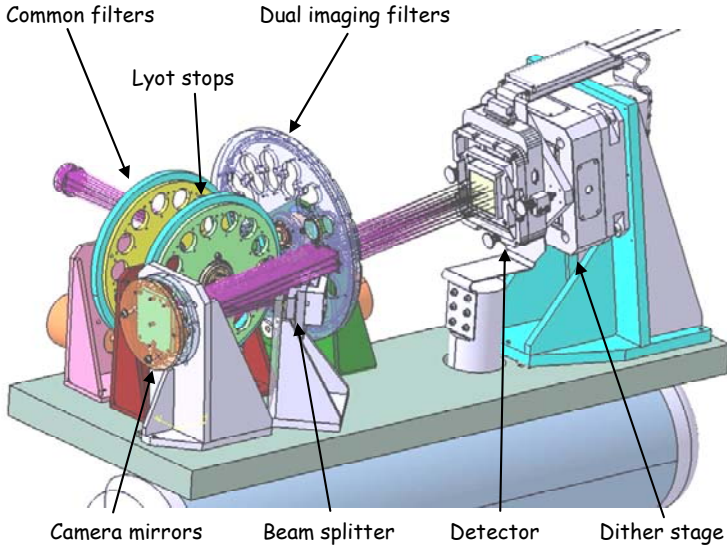


Figure 4. IRDIS opto-mechanical implementation (left) and the interior of the cryostat during integration (right).

3. MANUFACTURING

3.1. Optics and filters

Following a call for tenders, three companies have been chosen to provide most of the optical components for IRDIS. Winlight (France) provides all non-filter optics and substrates for broad and dual-band filters, Cilas (France) provides coating of broad and dual-band filters, and Omega (USA) provides narrow-band filters. In addition to these three large contracts, the grism is provided by Newport (USA), and polarizers are provided by Meadowlark (USA). We have so far received all optics and a few of the filters. The main difficulty of optics manufacture was foreseen to be the achievement of the nanometric wave front error specifications on all the optics in the differential path. This has been achieved, and with an estimated 6nm rms differential aberration, we are nearly reaching the goal performance of 5nm rms. Common aberrations in the imaging modes are below 30nm rms, well within the goal specification of 50nm.

Filters were early on identified as critical components for IRDIS because of their presence in the differential path. A prototype experiment^[15] was implemented to demonstrate that adequate wavefront quality could be reached, accounting for substrate polishing, coating in-homogeneity, and bending due to coating stresses. Other critical issues for the filters include out-of-band blocking capacity and in-band transmission rate. The blocking capacity is particularly critical in view of the extremely wide-band sensitivity of the detector, with nearly 100% quantum efficiency from the visible up to 1.7 μ m. A classical approach to blocking specification, fixing a hard limit of 1e-4 for out-of-band transmission, turned out to be prohibitive in terms of cost and even feasibility, requiring an unreasonably large number of thin film layers. Instead, we implemented a specification based on scientific requirements, defining two blocking integrals, one ensuring blocking of out-of-band starlight, the other concerning thermal flux.

The blocking integrals are calculated from $\lambda_L = 400\text{nm}$, $\lambda_H = 2700\text{nm}$, the limits of the detector sensitivity. Blocking integrals exclude the filter bandpass region between low and high cut-off wavelengths (λ_{CL} and λ_{CH}), defined as the points of 1% transmission. Stellar blocking, I_S , is calculated for a blue stellar object as the ratio between integrated blocking range flux and in-band flux:

$$I_S = \frac{\int_{\lambda_L}^{\lambda_{CL}} S \times T \, d\lambda + \int_{\lambda_{CH}}^{\lambda_H} S \times T \, d\lambda}{\int_{\lambda_{C-\Delta\lambda}}^{\lambda_{C+\Delta\lambda}} S \times T \, d\lambda}$$

where S is source spectrum, see Figure 5 (left), including instrument transmission and detector sensitivity, and T is filter transmission. The sharp edge below 1 μ m is due to the SPHERE dichroic beam splitter. Broad and narrow-band filters are specified to $I_S < 1\%$, while the dual-band filters are specified to $I_S < 0.4\%$ (goal 0.1%).

Thermal blocking, I_T , is defined as the integral of out-of-band thermal background flux from a 300K black-body filling the instrumental etendue. Its unit is photons/s/pixel. It is calculated as follows:

$$I_T = \int_{\lambda_L}^{\lambda_{CL}} B \times T \, d\lambda + \int_{\lambda_{CH}}^{\lambda_H} B \times T \, d\lambda,$$

where B is the background emission spectrum (photons/s/ μm /pixel, see Figure 5, right), including instrument transmission and detector sensitivity, and T is filter transmission. In view of the fact that we observe bright targets at short exposure times, generally below 10s, we accept a thermal background through the filters of 0.5ph/s/pix for all filters within the T, J, and H bands. For K band filters, the specification is set corresponding to the in-band thermal flux of each filter, up to 50ph/s/pix for the broad-band filter.

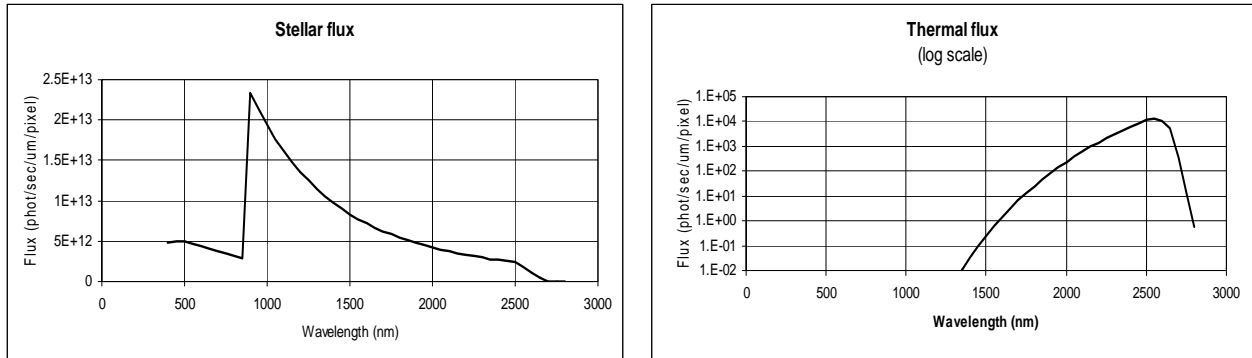


Figure 5. Source spectrum for calculation of stellar (left) and thermal (right) blocking.

Broad and dual-band filters are being manufactured by the Cilas company (France). To simplify the construction of the dual band filters, hence allowing to reach the stringent wavefront quality requirement by limiting the effect of spatial inhomogeneities in the coating, the blocking function of these filters is ensured by combining them with broad-band filters. This is possible since the latter are located in the common filter wheel, situated upstream of the beam separation optics. Separation of the blocking function from the band-pass definition also allows the use of high-grade fused silica for the dual-band filter substrates, further optimizing the quality of these filters. On the other hand, the short-wavelength blocking of broad-band filters is ensured by using absorbing substrate material, specifically the Schott colour glass RG 850 for the Y and J filters and silicon (Si) for the H and Ks filters. The dual-band filter coating stacks consist of multiple half-wave Fabry-Perot structures. The filters are manufactured using Dual Ion Beam Sputtering technology, leading to a dense microstructure of layers and high reproducibility of refractive indices. Layer thickness control is based on real-time in-situ optical monitoring and a quartz controller.

The narrow-band filters, all located in the common filter wheel, are being manufactured by the Omega company (USA). They apply a well-proven approach using two independent substrates glued together after coating, achieving perfect protection of the filter stacks deposited on internal surfaces by standard coating techniques. However, this process naturally introduces power to the filters since the bending of the substrates due to stress in the coating layers causes the glue layer to take on a lens shape. Although these filters are not as critical in terms of wavefront error as the dual-band filters, the requirement on optical quality is still much higher than usually encountered for such filters. A post-polishing process has therefore been implemented, allowing reduction of the power to an acceptable level.

3.2. Cryostat and cryogenic organs

The cryogenic design of IRDIS is based on the use of dual liquid nitrogen (LN2) tanks. A large tank with 60 litres capacity stores enough LN2 for at least 30h autonomy. It feeds a second, 10 litre capacity tank, mounted below the optical bench to which it is thermally connected by a series of copper braids. Since the second tank is permanently full, the thermal stability of the optical bench is maintained as long as there is a drop of LN2 left in the main tank. A thermal screen consisting of aluminium plates screwed onto the edges of the bench ensures a highly uniform thermal environment for the IRDIS optics. Radiative insulation of the screen and the LN2 tanks from the 300K cryostat wall is

achieved by the aid of a specially made multi-layer insulation (MLI) cover, see Figure 6. The main tank and the optical bench are both mounted to the cryostat base by hexapod structures. The hexapod rods are made of G10 epoxy in order to ensure thermal insulation.

Efficient cooling of the detector is provided through a copper rod plunged into the small LN2 tank and sticking up through a hole in the optical bench, see Figure 7. Special care is taken in the design of the soldered junction between this bar and the stainless steel tank in order to ensure tightness through numerous cooling cycles.



Figure 6. Manufacturing of the multi-layer insulation (MLI) coat (left image) and the coat covering the main LN2 tank and hexapod structure installed (right image).



Figure 7. The small LN2 tank (left image), known as the submarine, takes the form of a long cylinder situated under the optical bench. Cooling braids are fixed onto the wings. A copper rod provides cooling power to the detector. The design of the soldered junction between the rod and the stainless steel tank is made to ensure its viability through numerous cooling cycles (right image).

3.3. Mechanical mounts and mechanisms

The basic optical system of IRDIS consists of three fixed units, the beam splitter unit, the camera mirror unit, and the detector unit, separately aligned and mounted on the optical bench. The three filter wheels are mounted as two separate units, the common filter wheel and the Lyot stop wheel sharing a common base plate. All the units are first mounted and aligned on a dummy optical bench, allowing installation of the real optical bench, which is thermally and mechanically

coupled to the cryogenic system, into the cryostat independently of the optical alignment activities. When the alignment is ready and after bake-out and thermal acceptance of the cryostat, the optics units are transferred to the real optical bench, whose dowelled interfaces are identical to that of the dummy bench.

Space is scarce, and much care is taken in the design of the optical mounts to provide compact and stable mounts for the optics while at the same time implementing all necessary adjustment facilities. These are implemented in terms of support pads whose height can be finely adjusted by optical grinding, in order to ensure parallelism between the two output beams and differential defocus corresponding to a few nm rms wavefront error.

The interior of the instrument is blackened, either by inorganic black anodization (ESA standard ECSS-Q-ST-70-03C) or, for pieces too large for the anodization baths and for metals other than aluminium, by painting (MAP PU1). In both cases, hemispheric reflectance below 6% is maintained throughout the IRDIS spectral band. Note that classical organically dyed anodization reflects up to 60% in the 1-2 μ m range.

4. AIT

4.1. Status and test plans

As of June 2010, we have assembled the cryostat and checked its cryo-vacuum performances, and the thermal acceptance is scheduled for end of July 2010. All cables, filter wheel electronic control have been manufactured and tested. The filter wheels are assembled and tested at room temperature, and the validation of the mechanism control software is ongoing until the end of July. Except for the broad and dual-band filters that should be delivered in the fall of 2010, all IRDIS optics are now at LAM. Integration of optics into their mechanical mounts is ongoing and cryogenic alignment and wavefront verifications are foreseen in August and early September. IRDIS will then be fitted with most of its filters and undergo functional testing and detector alignment with its engineering-grade detector. Final optical performance verification and science performance characterization with the science-grade detector are scheduled for late fall 2010. We anticipate holding the IRDIS acceptance review by the end of the year.

A science test plan containing some 50 test procedures has been defined in order to validate the functionality and performance of IRDIS alone and as part of the SPHERE system in terms of instrument control and data processing capabilities, as well as calibration^[16] and operational strategies. In addition to debugging of the complete system, these tests are necessary in order to update the exposure time calculator (ETC) and to optimise observational efficiency and science return. The data volume produced during these tests will most likely be beyond 250 Gbytes.

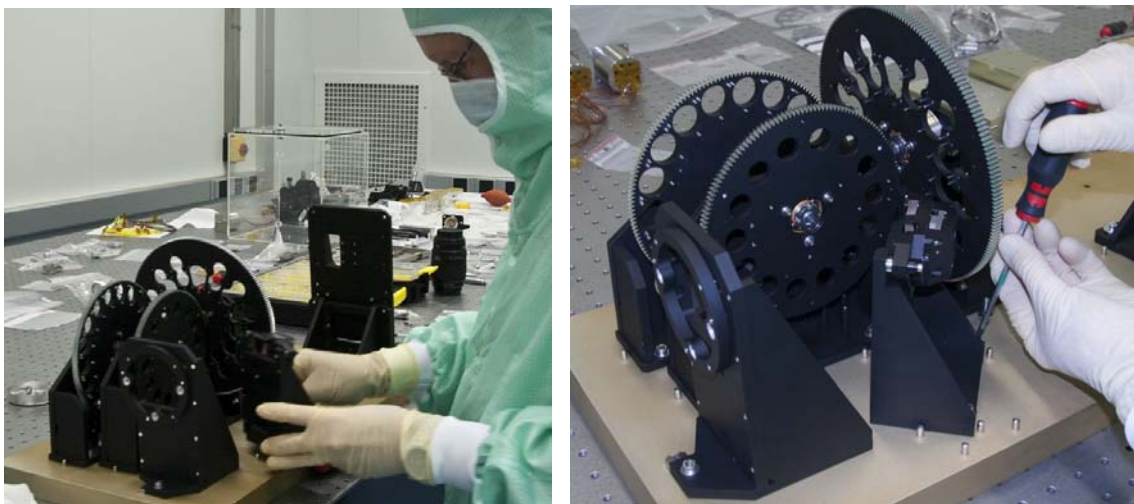


Figure 8. Installation of the optical and mechanical units on the dummy bench.

4.2. Detector tests

Two science grade detectors were tested for the Sphere instrument, one for IRDIS, the other for the IFS. These are two 2Kx2K Hawaii-2RG arrays manufactured by Teledyne Imaging Sensors. The CdZnTe substrates have been removed; this is now the standard array structure delivered by Teledyne, offering excellent quantum efficiency well into the visible and reduced sensitivity to cosmic rays. The detectors are operated with cryogenic preamplifiers located next to the focal plane and operating at temperatures of ~ 80 K. Data acquisition is done using the ESO-developed new generation controller (NGC) which reads all the 32 video channels of the Hawaii-2RG detectors in parallel.

These detectors are among the best Hawaii2RG detectors ever tested at ESO. Both detectors show excellent noise performance at the nominal operation temperature of ~ 80 Kelvin; read noise as low as 8 electrons for a normal double correlated read and down to 3 electrons for non destructive sampling has been measured. Quantum efficiency is extremely high over a broad band peaking from 96 to 100 % in J- Band, 96 to 97 % in H-Band and 86 to 89% in K-Band. Inter pixel coupling has been reduced compared to previous H2RGs tested at ESO with a maximum coupling of around 2% to the neighbouring pixels. Dark current is low and will allow a read noise limited detector performance in Sphere.

While the cosmetic quality of both detectors fulfils the specifications for science grade devices, this is the only point where some significant difference between the two detectors has been seen. One of the devices (#226) is found to suffer from a hand-full of bad-pixel clusters with a typical diameter of 20 pixels. Such clusters are not present in the other device (#218), but this one has more numerous isolated hot pixels. While the presence of clusters will have a serious impact on the quality of spectral images in the IFS, they are judged acceptable in the case of IRDIS thanks to the continuity of the IRDIS images. Moreover, since IRDIS only uses half the detector area, it is possible to select the best part of the detector, hence avoiding most of the clusters, see Figure 9.

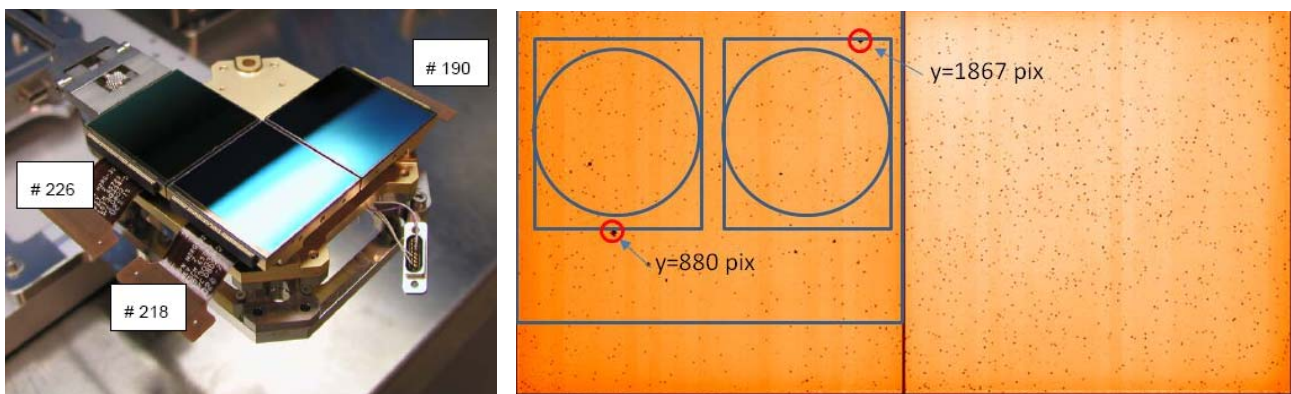


Figure 9. Mounting of detectors during the tests (left image). Flat field map of the two science detectors (right image), #226 to the left, #218 to the right. The chip #226 has less isolated bad pixels but some clusters, some of which can be avoided by shifting the IRDIS FOV somewhat (~ 6 mm) off-center, as shown.

4.3. Mechanism tests

The IRDIS instrument contains three wheel mechanisms working at cryogenic temperature. The most demanding filter wheel requires a position repeatability of $10\mu\text{m}$ ($20''$) for a position changing time of 5s. The wheel was designed so that one motor turn corresponds to one filter change, this greatly simplifies the control architecture. Indeed only two sensors are used to drive the wheel; one, placed at the motor shaft, checks that the position is correct, the other, placed on the wheel, serves as home sensor. Given the high repeatability required, a lock mechanism was originally designed to maintain the wheel in position, but it was not clear to what extent such a lock would be necessary. The cost of the lock device was considerable complexity, both in terms of mechanical design and control-command, but also in terms of filter switching delay. The filter change sequence consisted in moving the lock device, verify that the lock is free with a dedicated sensor, move the wheel using main motor, verify that the position is correct and then move the lock to clamp the wheel. Without the lock device the sequence consists in moving the motor the required number of steps, then verifying that the motor has arrived to a filter position using the sensor at the motor shaft.

A cryogenic prototype mechanism was developed and extensively tested to evaluate the performance of the wheel and to study the need for a locking device. It was found that the required positioning accuracy was achieved in both cases, but the switching time, nearly a factor two longer with the lock than without, could only be achieved without the lock. As shown on Figure 11, a repositioning stability of $\pm 3\mu\text{m}$ is obtained for the filter wheel without using the lock device. This performance was achieved without any holding current, the torque of the unpowered motor being sufficient to guarantee the stability. This point is important, allowing to minimize the motor power dissipation hence avoid excessive LN2 consumption. A maximum filter changing time of around 3.5s was established.

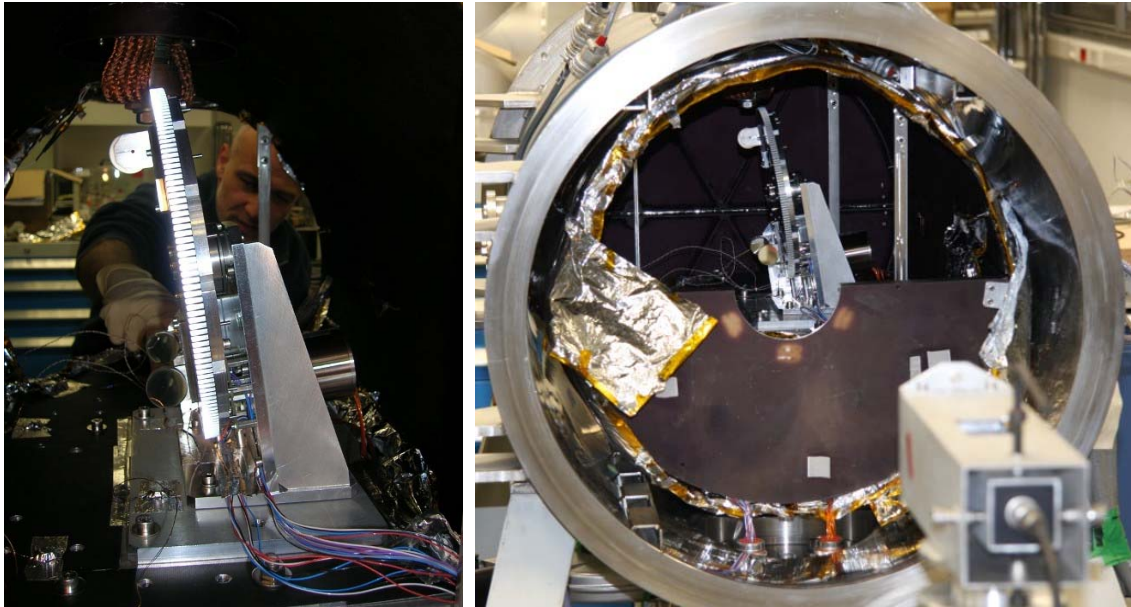


Figure 10 Filter wheel prototype during installation within the test cryostat.

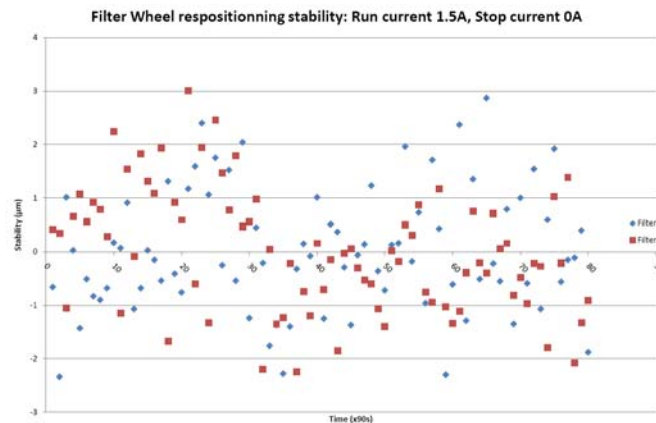


Figure 11 Filter wheel repositioning stability at cryogenic temperature

4.4. Cryo-vacuum functional tests

Qualification of the cryogenic system of IRDIS is currently ongoing. Vacuum and leakage tests have been done, and the first LN2 filling, verifying cool-down curves and LN2 autonomy have been conducted successfully, see Figure 12. The LN2 valve was opened 4 hours after starting the pump-down, and the tanks were full 6.5h later. A stable temperature of the optical bench was reached in less than 15h, far quicker than the required 25h. After 31h cold, the heaters were switched on. At this point, the main LN2 tank was still more than 1/3 full, indicating that the 30h autonomy requirement was reached with good margin.

The main test still remaining is the test of the detector thermal environment, allowing qualification of the detector operating temperature, required to be at around 80K, and to make sure the cool-down and warm-up conditions are safe. To avoid contamination of the detector during transients, it is required to be maintained warmer than its surroundings during these operations. While basic cryostat design should ensure this passively, a dedicated heater has been designed to allow thermal regulation if necessary. This test will be done with all detector hardware installed, apart from the detector chip itself.

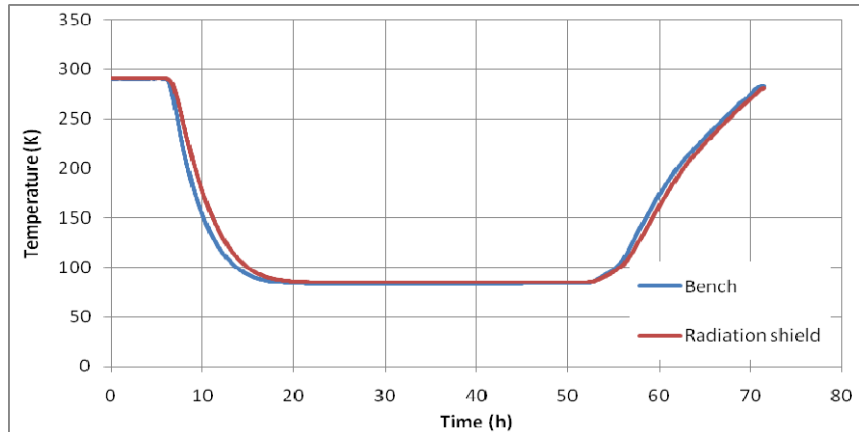


Figure 12. Temperature profile of the optical bench and the radiation shield during the first cool-down of the cryostat.

5. CONCLUSION

We have described the IRDIS science module of SPHERE, a planet finding instrument for the ESO VLT observatory, in terms of its system design and in view of its science goals and expected performances. The instrument relies upon a state-of-the-art extreme AO system for compensation of atmospheric turbulence and instrumental aberrations, highly performing coronagraphs to minimize diffracted starlight, and high-quality dual imaging hardware associated with highly evolved image analysis software. IRDIS provides several modes including dual band and dual polarization differential imaging, and low and medium resolution long-slit spectroscopy through the near infrared bands from 950 to 2320nm. At 1600nm it is expected to reach a 5σ contrast of $\sim 2 \cdot 10^{-5}$ at its inner working angle of 100mas, and $\sim 5 \cdot 10^{-7}$ at 600mas.

ACKNOWLEDGEMENTS

SPHERE is an instrument designed and built by a consortium of French, German, Italian, Swiss and Dutch institutes in collaboration with ESO.

REFERENCES

- [1] Beuzit, J.-L., Feldt, M., Dohlen, K., Mouillet, D., Puget, P., Antichi, J., Baruffolo, A., Baudoz, P., Berton, A., Boccaletti, A., Carillet, M., Charton, J., Claudi, R., Downing, M., Feautrier, P., Fedrigo, E., Fusco, T., Gratton, R., Hubin, N., Kasper, M., Langlois, M., Moutou, C., Mugnier, L., Pragt, J., Rabou, P., Saisse, M., Schmid, H. M., Stadler, E., Turrato, M., Udry, S., Waters, R., and Wildi, F., "SPHERE: A 'Planet Finder' Instrument for the VLT," *The Messenger* 125, 29–34 (2006).
- [2] Dohlen, Kjetil; Beuzit, Jean-Luc; Feldt, Markus; Mouillet, David; Puget, Pascal, et al., "SPHERE: A planet finder instrument for the VLT," in: *Ground-based and Airborne Instrumentation for Astronomy*. McLean, Ian S.; Iye, Masanori. Eds., Proc. SPIE, Volume 6269, pp. 62-69 (2006).
- [3] T. Fusco, C. Petit, J.-F. Sauvage, G. Rousset, M. Kasper, K. Dohlen, J. Charton, P. Rabou, P. Feautrier, P. Baudoz, J.-L. Beuzit, M. Downing, E. Fedrigo, D. Mouillet, P. Puget, "Design of the extreme AO system for the planet-

- finder instrument of the VLT," in *Advances in Adaptive Optics II*, Brent L. Ellerbroek, Domenico Bonaccini, eds, Proc. SPIE 6272 (2006).
- [4] Anthony Boccaletti, Lyu Abe, Jacques Baudrand, Jean-Baptiste Daban, Richard Douet, Geraldine Guerri, Sylvie Robbe-Dubois, Kjetil Dohlen, and Dimitri Mawet, "Prototyping coronagraphs for exoplanet characterization with SPHERE," Proc. SPIE 7015 (2008).
 - [5] Dohlen, Kjetil; Langlois, Maud; Saisse, Michel; Hill, Lucien; Origne, Alain; Jacquet, Marc; Fabron, Christophe; Blanc, Jean-Claude; Llored, Marc; Carle, Michael; and 6 coauthors, "The infra-red dual imaging and spectrograph for SPHERE: design and performance," Proc. SPIE 7014, p. 70143L (2008).
 - [6] De Caprio, V., Giro, E., Claudi, R., et al. "Manufacturing and integration of the IFS integral spectrograph for SPHERE," Proc SPIE 7735 (2010).
 - [7] Roelfsema, R., Bazzon, A., Pragt, J., Schmid, H. M., et al., "The ZIMPOL high-contrast imaging polarimeter for SPHERE: design, manufacturing, and testing," SPIE Conf. Vol. 7735, (2010).
 - [8] Racine, R., Walker, G. A. H., Nadeau, D., Doyon, R., & Marois, C., "Speckle Noise and the Detection of Faint Companions," PASP, 111, 587 (1999).
 - [9] Cavarroc, C.; Boccaletti, A.; Baudoz, P.; Fusco, T.; Rouan, D., "Fundamental limitations on Earth-like planet detection with extremely large telescopes," *Astron. Astrophys.* 447, (2006), pp.397-403.
 - [10] M. Langlois, K. Dohlen, H-M. Schmid, J.-C. Augereau, D. Mouillet, "NIR polarimetry with SPHERE-IRDIS", Proc SPIE 7735 (2010).
 - [11] Vigan, A.; Moutou, C.; Langlois, M.; Allard, F.; Boccaletti, A.; Carbillet, M.; Mouillet, D.; Smith, I., "Photometric characterization of exoplanets using angular and spectral differential imaging", *MNRAS* 924 (2010).
 - [12] Vigan, A.; Langlois, M.; Moutou, C.; Dohlen, K., "Exoplanet characterization with long slit spectroscopy", *A&A* 489, 1345 (2008).
 - [13] Vigan, A.; Moutou, C.; Langlois, M.; Mouillet, D.; Dohlen, K.; Boccaletti, A.; Carbillet, M.; Smith, I.; Ferrari, A.; Mugnier, L.; Thalmann, C., "Comparison of methods for detection and characterization of exoplanets with SPHERE/IRDIS", Proc. SPIE 7735 (2010).
 - [14] Ralf-Rainer Rohloff, Thomas Blümchen, Markus Feldt, Vianak Naranjo, Jose Ramos, Klaus-Dieter Müller, Harry Marth, Patrick Pertsch, Kjetil Dohlen, "A cryogenic dithering stage for moving SPHERE-IRDIS' detector," Proc. SPIE 7018 (2008).
 - [15] Kjetil Dohlen, Michel Saisse, Alain Origne, Gabriel Moreaux, Christophe Fabron, Frederic Zamkotsian, Patrick Lanzoni, Frederic Lemarquis, "Prototyping of differential optics for the IRDIS dual imaging camera for the SPHERE planet finder instrument," Proc. SPIE 7018 (2008).
 - [16] M. Langlois, A. Vigan, D. Mouillet, C. Moutou, "Impact of calibration on performance for extrasolar planets direct imaging with the infrared dual-imaging camera and spectrograph for SPHERE", Proc SPIE 7735 (2010).